Effective Synthesis and Biological Evaluation of Natural and Designed Bis(indolyl)methanes via Taurine-Catalyzed Green Approach

Kailas A. Chavan,[#] Manjari Shukla,[#] Amar Nath Singh Chauhan,[#] Sushobhan Maji, Ghanshyam Mali, Sudipta Bhattacharyya,* and Rohan D. Erande*
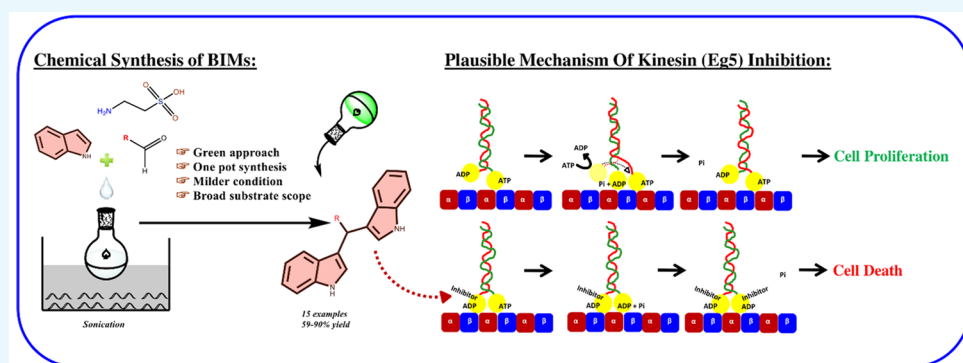
Read Online

ACCESS | Metrics & More | Article Recommendations | SI Supporting Information

ABSTRACT: An ecofriendly, inexpensive, and efficient route for synthesizing 3,3′-bis(indolyl)methanes (BIMs) and their derivatives was carried out by an electrophilic substitution reaction of indole with structurally divergent aldehydes and ketones using taurine and water as a green catalyst and solvent, respectively, under sonication conditions. Using water as the only solvent, the catalytic process demonstrated outstanding activity, productivity, and broad functional group tolerance, affording the required BIM natural products and derivatives in excellent yields (59−90%). Furthermore, in silico based structure activity analysis of the synthesized BIM derivatives divulges their potential ability to bind antineoplastic drug target and spindle motor protein kinesin Eg5. The precise binding mode of BIM derivatives with the ATPase motor domain of Eg5 is structurally reminiscent with previously reported allosteric inhibitor Arry520, which is under phase III clinical trials. Nevertheless, detailed analysis of the binding poses indicates that BIM derivatives bind the allosteric pocket of the Eg5 motor domain more robustly than Arry520; moreover, unlike Arry520, BIM binding is found to be resistant to drug-resistant mutations of Eg5. Accordingly, a structure-guided mechanism of Eg5 inhibition by synthesized BIM derivatives is proposed.

INTRODUCTION

3,3′-Bisindolylmethane (BIM) and its functionalized class of natural products were originally isolated from cruciferous plants and terrestrial and marine organisms and shown to contain a broad array of medicinal properties.[1−3] Key members of this class of natural products include arundine, vibrindole A, streptindole, arsindoline A, tris(1*H*-indol-3-yl)methane, and trisindoline (Figure 1).[4−10] A unique structure of this bioactive intermediate contains two indole units which are responsible for exhibiting a range of essential biological activities such as anti-neurodegenerative, anti-inflammatory, anticancer, antibiotic, insecticidal, antimicrobial, antifungal, and antioxidant properties (Figure 1).[7,11−20] Interestingly, some of these BIM derivatives are used as a sedatives in the treatment of AIDS, chronic fatigue, irritable bowel syndrome, and cancer, while bis(indolyl)arylmethane-bearing compounds are used as drugs for Parkinson's disease, obesity, and bacterial and oncolytic

viruses.[18,21−29] In addition, BIMs have also been found to have the potential to normalize abnormal cell growth associated with cervical dysplasia.[30]

Moreover, BIMs have grown in prominence in recent years, particularly after the discovery of their effective involvement in suppressing prostate cancer cells in humans.[31,32] Because of their impressive pharmaceutical properties coupled with their high demand in medicinal chemistry, drug discovery, and agrochemicals, BIMs have become a frequent target for synthetic organic chemists worldwide, and intense research
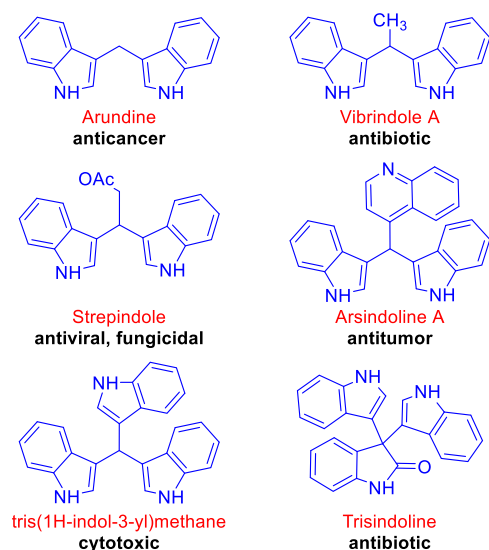
Figure 1. Representative analogues of naturally occurring 3,3′-BIMs with relevant bioactivity.

activities toward their structural modification and biological evaluation have been pursued. As a result of this surge, numerous methods have been devised for the production of naturally occurring BIMs and their functionalized analogues (see Scheme 1).[7,11,33,34] Interestingly, most methods utilize 3-

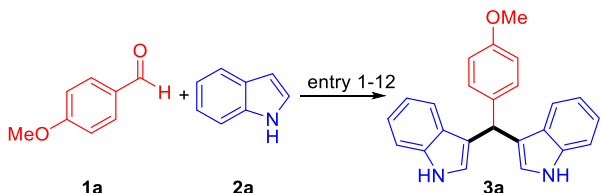**Scheme 1. Synthesis of Symmetrical and Unsymmetrical BIMs**
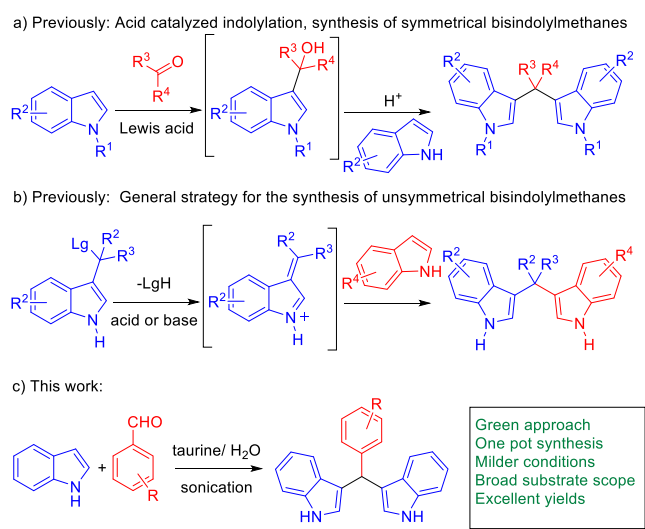
indole aromatic alcohols to afford symmetrical and unsymmetrical 3,3′-BIMs using a condensation strategy with appropriate nucleophiles.[19,35] In addition, the most common reaction protocols used in the synthesis include expensive and excess amounts of catalysts such as Cu-catalysts,[36] TsOH, Ga(OTf)$_3$, Zn(OTf)$_2$, etc.[37−39] Several catalytic pathways were also developed to afford BIMs, which includes Bronsted or Lewis acid, methanol, iodine, electrolysis methods, metal salts, visible light, and enzymes.[40−42] Moreover, solid acidic catalysts such as Amberlyst, montmorillonite clay K-10, TiO$_2$, ZrOCl$_2$/SiO$_2$, HClO$_4$−SiO$_2$, and P$_2$O$_5$/SiO$_2$ have also been investigated so far.[43−46] Over the last decades, methods for fabricating symmetrical and unsymmetrical 2,3′- and 3,3′-

BIMs have primarily focused on the indolylation of 3-indolylmethyl alcohol, sulfone, malononitrile, 2,4,6-trimethox-ybenzene, etc. with indole derivatives.[47−51] Although the divulged methodologies are phenomenal, they have some downsides, such as the need for expensive and higher catalytic loading, harsh reaction conditions, time-consuming reaction procedures, use of hazardous organic solvents, inadequate yields, and a constrained substrate scope. Considering an excellent medicinal profile and necessity, BIMs always demand a scalable method and new functionalized analogues for further drug discovery and development. As a corollary, there is an undeniable potential for an efficient and environmentally friendly approach to synthesize BIMs.
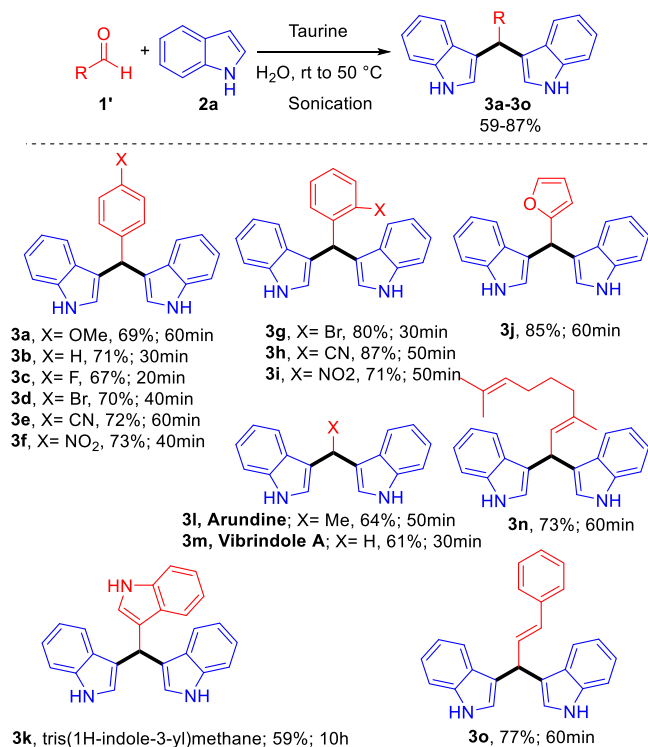
Herein, with an aim toward developing potential therapeutic antineoplastic leads, we set out to optimize an ecofriendly one-pot organic synthesis method to obtain naturally occurring potent BIMs along with their novel derivatives targeting crucial cancer drug leads. Therefore, in continuation of our unwavering interest in indole compounds,[52−54] we investigated the chemistry of condensation of indoles with aldehydes and ketones catalyzed by taurine (C$_2$H$_7$NO$_3$S) using only water as a green solvent.[55] As part of our effort to overcome drawbacks from the previous report and formulate an efficient green approach, we describe here a combination technique of sonication and aqueous media at a moderate temperature. The described synthetic approach culminated into a simple, ecofriendly, one-pot methodology that produces 17 desired BIM derivatives including four natural products, arundine, vibrindole A, tris(1H-indol-3-yl)methane, and trisindoline, in high yields with no transitional isolation. Considering the myriad applications of BIM derivatives in several anticancer therapies, we conducted in silico structure activity analysis of the synthesized BIM derivatives against anticancer drug targets. In this context, mitotic kinesin Eg5 is an alluring target for antineoplastic drugs as it plays a pivotal role in the formation and stabilization of bipolar spindle architecture and faithful chromosomal segregation.[56−58] Kinesin Eg5 is a multidomain molecular machine that transforms ATP-driven mechanochemical force to glide unidirectionally on a microtubule track through a series of motor domain conformational changes and associated changes in microtubule affinities.[59−61] Intriguingly, the synthesized BIM derivatives were found to dock at one of the well-established allosteric inhibitor (monastrol) binding sites of the Eg5 motor domain which also houses two other distinct allosteric inhibitor-binding sites.[62−64] The monastrol binding allosteric site offers high target specificity but suffers from the emergence of recently reported drug-resistant mutations (D130A and L214A).[65] Hence, since the discovery of monastrol site targeting resistance, resistant therapeutic leads are in high demand to confront drug-resistant Eg5 mutations.[66] Interestingly, the synthesized BIM derivatives were found to be recalcitrant toward drug-resistant Eg5 mutations. The detailed structure activity analysis of BIM derivative(s)/Eg5 binding and a plausible molecular mechanism of inhibition are presented herein.
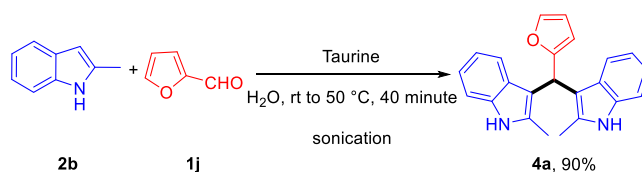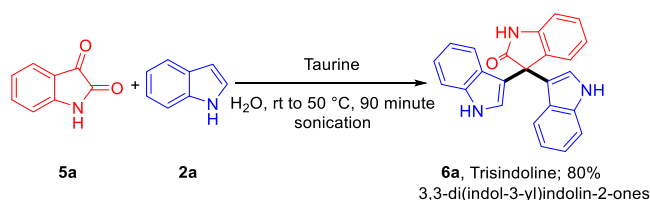
■ RESULT AND DISCUSSION

Being inspired by the green approach of BIMs synthesis methodology, and our recent report on the taurine-catalyzed multicomponent reaction for the synthesis of densely substituted dihydropyrano[2,3-c]pyrazoles,[66] we became interested in assessing the efficacy of taurine as a catalyst to boost the multicomponent reaction of probe indole and function-

Table 1. Selected Optimization Studies to Access BIMs and Analogues: Effect of Different Supports[a]

| entry	catalyst[b]	solvent[c]	temp (°C)	time (h)	yield[d] (%)
1	Cu(OTf)$_2$	CH$_2$Cl$_2$	23	16	50
2	Cu(OTf)$_2$	CH$_2$Cl$_2$	50	10	44
3	BF$_3$·OEt$_2$	CH$_2$Cl$_2$	23	4	34
4	taurine	CH$_2$Cl$_2$	23	20	52
5	taurine	H$_2$O	23	24	trace
6	taurine	H$_2$O	50	24	trace
7[e]	taurine	H$_2$O	23	24	trace
8[e]	taurine	H$_2$O	50	24	trace
9[f]	taurine	H$_2$O	23	2	60
10[f]	**taurine**	**H$_2$O**	**50**	**1**	**69**
11[e,f]	taurine	H$_2$O	50	1	54
12[f]	no catalyst	H$_2$O	50	24	trace

[a]Reaction conditions: aldehyde (1.0 mmol) and indole (2.0 mmol). [b]Catalyst: 5 mol %. [c]Solvent: 3−5 mL. [d]Isolated yields based on starting material recovered. [e]Catalyst: 10 mol %, [f]Sonication.

Scheme 2. Taurine-Catalyzed One-Pot Synthesis of BIM Derivatives

3a, X= OMe, 69%; 60min
3b, X= H, 71%; 30min
3c, X= F, 67%; 20min
3d, X= Br, 70%; 40min
3e, X= CN, 72%; 60min
3f, X= NO2, 73%; 40min

3g, X= Br, 80%; 30min
3h, X= CN, 87%; 50min
3i, X= NO2, 71%; 50min

3j, 85%; 60min

3l, Arundine; X= Me, 64%; 50min
3m, Vibrindole A; X= H, 61%; 30min

3n, 73%; 60min

3k, tris(1H-indole-3-yl)methane; 59%; 10h

3o, 77%; 60min

Scheme 3. Synthesis of Indole-Functionalized BIM Derivative

Scheme 4. Synthesis of Trisindoline: Spiro-analogue 3,3-Di(indol-3-yl)indolin-2-ones

methylene)bis(1H-indole) **3a**, and the results are summarized in Table 1. Initially, to understand the role and effect of Lewis acid as a catalyst, reactions of aldehyde **1a** and indole **2a** were examined under different solvents and temperatures to afford **3a**. As a result, the reaction was found to be very slow with a catalytic amount of Cu(OTf)$_2$ in DCM at room temperature to 50 °C and afforded only 50% and 44% yield, respectively (see entries 1 and 2, Table 1). Similar findings were observed with BF$_3$·OEt$_2$, where the reaction time was greatly decreased but the yield was reduced to 34%, (see entry 3, Table 1). To our delight, the reaction with the newly implemented catalyst taurine proceeded smoothly in CH$_2$Cl$_2$ at room temperature to afford BIMs **3a** selectively in 20 h with 52% yield (see entry 4, Table 1). However, opposite results were observed when the reaction was performed in water medium leading to only a trace amount of compound (entry 5, Table 1). Notably, an increase of the reaction temperature from 23 to 50 °C or increase of catalyst loading from 5 to 10 mol % did not furnish the required product in an isolable yield (see entries 6−8, Table 1). Interestingly, the taurine-catalyzed combination technique of sonication and aqueous media delivered the required product in 60% yield (see entry 9, Table 1). Remarkably, the highest yield of 69% was obtained when the reaction was performed at 50 °C using the taurine-catalyzed sonication reaction in water medium (see entry 10, Table 1). In order to establish the conditions, the reaction was attempted with an excess catalyst but did the yield did not increase (see entry 11, Table 1). It is worth mentioning that an attempt was made to validate the sonication conditions by changing the reaction temperature, catalyst loading, and time but keeping water as a green solvent did not improve the yield, favoring sonication as a necessary condition (see entries 5−8, Table 1). Moreover, to verify the need of a catalyst, a trial was conducted without any catalyst, in which all of the components were sonicated in H$_2$O at 50 °C for 24 h, which led to no product formation; hence, the requirement of the catalyst was confirmed for the reaction (see entry 12, Table 1). Most of the catalytic pathways employed to reach BIMs derivative **3a** yielded positive results, as shown in Table 1, but the best results were obtained with taurine-catalyzed water-mediated reaction at 50 °C that gave 69% yield (see entry 12, Table 1). Further, to demonstrate the generality of developed method, the protocol was expanded to synthesize functionalized BIMs

alized aldehyde. In our quest to find a best catalytic condition to access BIMs and their derivatives, the reaction was performed with p-methoxybenzaldehyde **1a** and indole **2a** as a model substrate under a different set of catalysts and conditions. Thus, a mixture of aldehyde **1a** (1 mmol) and indole **2a** (2 mmol) was treated under various solvent and catalytic conditions to afford 3,3′-((4-methoxyphenyl)-

Scheme 5. Plausible Reaction Mechanism for Synthesis of 3,3′-((4-Methoxyphenyl)methylene)bis(1*H*-indole) 3a
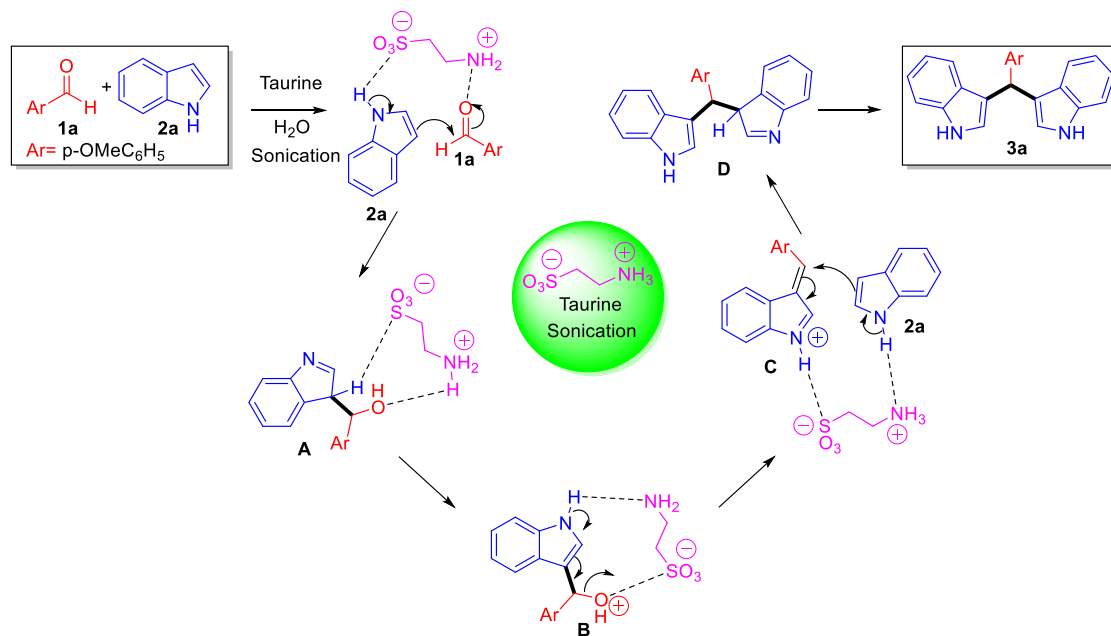
by treating the indole with a range of aldehydes, and the findings are reported in Scheme 2. Interestingly, the reactions of indole (2.0 equiv) with varying aldehydes (1.0 equiv) under the optimized conditions proceeded smoothly and resulted in the newly designed products **3b–3o** in 59−87% yield (see Scheme 2). The developed strategy was well-tolerated for both the aromatic aldehydes (**1a–1i**) and aliphatic aldehyde (**1l–1n**) to construct 17 designed bis(indolyl)methanes including four naturally occurring BIMs called arundine, vibrindole A, tris(1*H*-indol-3-yl)methane, and trisindole in excellent yields. Moreover, aromatic aldehydes **1a** possessing an electron-donating group (−OMe) and (**1c–1i**) possessing electron-withdrawing groups (F, Br, CN, NO$_2$) afforded the corresponding product in excellent yield (67−87%; Scheme 2). Furthermore, the approach was tested for heterocyclic aldehydes **1j,k**, and to our delight, both reactions operated well without producing any side products. Next, we aimed to establish a new BIM derivative **4a** utilizing a substituted indole skeleton to further investigate the extent of the proposed catalytic system. As a result, biochemical precursor 2-methylindole **2b** processed with furfural **1j** at taurine produced the optimal sonication conditions.

Intriguingly, the reaction proceeded very well and produced the required core in 90% yield in about 40 min (see Scheme 3). We were indeed inspired by the outcomes and next turned our attention to the development of innovative spiro-analogues 3,3-di(indol-3-yl)indolin-2-ones **6a**. Thus, we opted to replace the aldehyde moiety with the bioinspired group isatin **5a** in view of obtaining a novel spiro-analogue of the BIM framework. The bioinspired natural product isatin belonging to plants and humans is well-known for its presence in many bioactive compounds and their spiro-congeners and is responsible for a broad array of biological activities such as antiviral, anti-HIV, antitumor, and antitubercular properties.[67−69] Interestingly, taurine-catalyzed water-mediated sonication reaction of indole **2a** with isatin **5a** under the optimized conditions furnished a well-designed fused spirooxindole product 3,3-di(indol-3-yl)indolin-2-one **6a** with 80% yield (Scheme 4). In comparison to other functionalized aldehydes,

the ketone component of isatin shows a sluggish reactivity. The structure of all of the synthesized BIMs analogues **3a-o**, **4a**, and **6a** were validated unambiguously from their spectroscopic investigation (^{1}H NMR, ^{13}C NMR, IR, HRMS and melting point) (see the Supporting Information for details). As a result of the wide functional group tolerance and extremely effective catalytic support, numerous targeted varied BIMs were synthesized and further screened for their biological evaluation.

Plausible Mechanism. A plausible reaction mechanism for the water mediated taurine-catalyzed green multicomponent reaction of indole **2a** and *p*-methoxy benzaldehyde **1a** is depicted in Scheme 5. The catalyst used here is taurine, a naturally occurring *β*-amino sulfonic acid (pK_a = 1.5) that appears to be in zwitterion form when dissolved in water. Thus, taurine behaves as a bifunctional donor−acceptor reagent that facilitates the electrophilic substitution reaction by activating the carbonyl electrophilic site, which is then functionalized by the desired nucleophile.[70,71]

As a result, the taurine-activated aldehyde **1a** moiety was apparently invite the activated indole **2a** through an addition reaction leading to adduct **A**. In the presence of taurine, intermediate **A** experienced protonation followed by dehydration to form another intermediate benzylidene-3*H*-indole **C** via intermediate **B**; subsequently, the next activated indole **2a** facilitated the formation of bis indole moiety **D**, which underwent an imine−enamine tautomerization to deliver the targeted BIM derivative **3a**.

Biological Evaluation. Initial ligand-based target identification studies indicate that synthesized BIM derivatives efficiently bind three potential anticancer drug target proteins. Analysis of the free energy of binding (ΔG) for each of these drug target proteins clearly suggests high binding affinities for the synthesized BIM derivatives (Supplementary Table S1).

Intriguingly, among these three potential anticancer drug target proteins, the synthesized BIM derivatives were found to bind at the allosteric drug binding pocket of mitotic Kinesisn Eg5 (PDB id: 2PG2). On the contrary, the BIM derivative binding hotspots for the other two anticancer drug target proteins [Human p38 *α* MAP Kinase (PDB Id: 3HVC) and
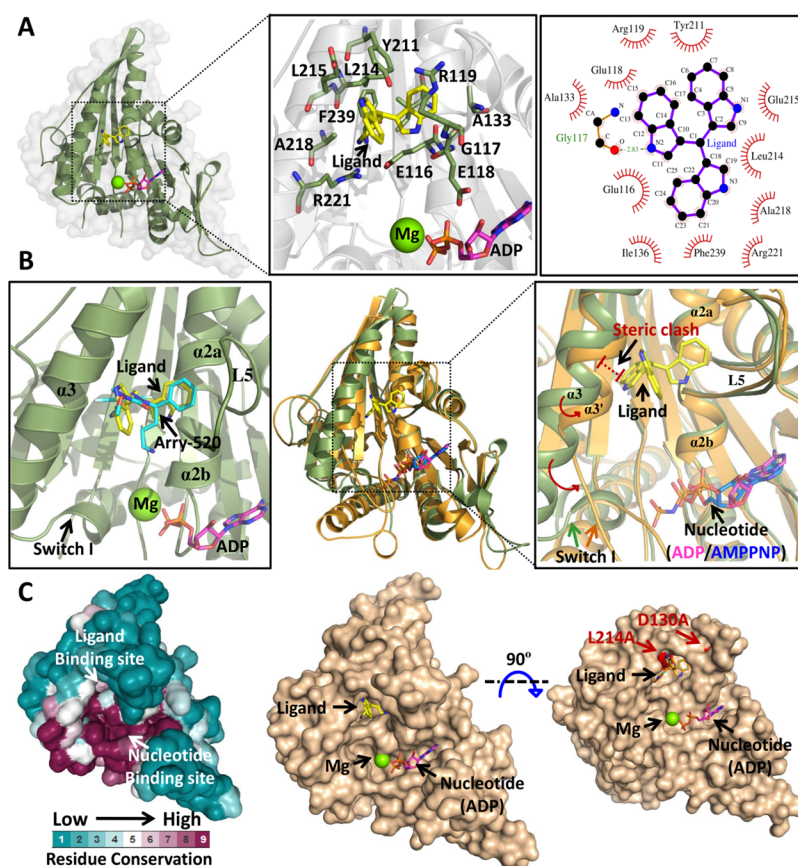
Figure 2. Plausible role of synthesized BIM derivatives as the monastrol site targeting allosteric inhibitor of mitotic kinesin Eg5. (A) Molecular docking of BIM derivative **3k** with the motor domain of Eg5 kinesin. The left panel shows the position of the docked ligand at the monastrol binding allosteric site of Eg5. The middle panel emphasizes the three-dimensional interaction pattern of bound ligand **3k** with the monastrol binding allosteric site amino acid residues of Eg5. The right panel shows the detailed two-dimensional interaction profile of the docked ligand **3k** with the monastrol binding allosteric site amino acid residues of Eg5. Green dotted line represents the formation of the hydrogen bond. Spiked arches represent hydrophobic interactions. (B) Plausible **3k**-mediated inhibition mechanism of Eg5 kinesin in comparison with the well-established allosteric inhibitor Arry520. The left panel shows that the cocrystallized allosteric inhibitor Arry520 and the synthesized BIM derivative **3k** targets the same inhibitory site of Eg5. The middle panel and the right panel show the structural superimposition of **3k** docked and ADP bound state of Eg5 (colored forest green) with its AMPPNP (ATP analogue) bound state (colored golden yellow). In the right panel, the zoomed view of the superimposed allosteric site clearly indicates that **3k** binding will hinder the structural transition from ADP to ATP bound conformational states of Eg5. (C) Bonastrol targeting allosteric site of Eg5 kinesin is not highly conserved. Left panel shows the site-specific evolutionary rates of Eg5 kinesin motor domain mapped on its structure surface and color coded from purple (highly conserved sites) to deep cyan (least conserved sites). The middle and the right panels show the positions of recently reported drug-resistant point mutations of Eg5 with respect to the **3k** binding site and the nucleotide binding site.

Table 2. *In Silico* Molecular Docking Based Binding Energy Estimation of Synthesized Bis(indolyl)methane Derivatives with the Motor Domain of Mitotic Kinesin Eg5 and Its Recently Reported Drug-Resistant Point Mutant Variants

| | binding energy (ΔG) | | |
| | | drug-resistant Eg5 mutants | |
bis(indolyl)methane derivatives	WT Eg5 kinesin (kcal/mol)	D130A (kcal/mol)	L214A (kcal/mol)
3k	−11.2	−11.1	−10.5
3b	−11.2	−11.0	−9.7

Human 3 alpha HSD type 3 (PDB id: 1J96)] were found to be located at the active site clefts (data not shown) of the respective enzymes, indicating a probabilistic substrate competitive mode of inhibition. Compared to substrate competitive inhibitors, allosteric inhibitors are always in high demand as they can offer more target specificity and thereby less associated side effects. Moreover, mitotic kinesin Eg5 is

one of the most well-established anticancer drug targets explored so far. Inhibition of Eg5 leads to mitotic arrest and apoptosis in neoplasms.[62] Among the three novel allosteric drug binding sites of Eg5 motor domain, the monastrol binding site is the most well characterized allosteric inhibitor binding site. A few monastrol binding site targeting Eg5 inhibitors are already in advanced stages of clinical trials,[63] although the fate of those inhibitors is ambiguous as the monastrol binding site of Eg5 kinesin suffers from moderate to low amino acid conservation compared to the nucleotide binding site (Figure 2C, all panels). In particular, owing to the emergence of specific drug-resistant mutations (D130A and L214A), the therapeutic future of monstrol binding site targeting allosteric inhibitors is uncertain.[64] Interestingly, the synthesized BIM derivatives **3k** and **3b** also dock at the same monastrol binding site, which is at the interface of α3 helix, α2 helix, and Loop 5 (L5) of the Eg5 motor domain (Figure 2A, all panels, and Figure 2B, leftmost panel). The common **3k** and **3b** binding sites are approximately 12 and 10 Å away from the

nucleotide binding site and catalytic Mg^{2+} binding sites of the Eg5 motor domain, respectively. The binding mode of docked BIM derivative **3k** is structurally reminiscent of the crystal structure of allosteric inhibitor Arry520 (commercial name Filanesib; targets Eg5 monastrol binding site) (PDB id: 6hky). Arry520 is currently under an advanced stage of clinical trials for treatment of multiple myeloma.[72] In order to compare the binding efficiency of synthesized BIM derivatives **3k** and **3b** with Arry-520, we docked the Arry520 molecule using the same docking platform and parameters used to dock BIM derivatives. The docked conformation of the Arry520 molecule was found to superimpose well with the published crystal structure (Supplementary Figure 2, all panels). Intriguingly, the comparative analysis of free energy of binding (ΔG) clearly indicates the synthesized BIM derivatives bind more efficiently at the same allosteric site of the Eg5 motor domain compared to Arry-520 ($\Delta G_{\text{Arry-520}} = -8.3$ kcal/mol versus $\Delta G_{3k} = -11.2$ kcal/mol; $\Delta G_{3b} = -11.2$ kcal/mol). Moreover, **3k** binding was found to be unaltered in the presence of the recently reported drug resistant variants (D130 and L214A) of Eg5 (Table 2). The highly efficient binding of BIM derivatives **3k** and **3b** at the allosteric drug binding pocket of Eg5 could be exemplified by the extensive array of hydrophobic interactions of the bound ligands with amino acid side chains of $\alpha 2,\alpha 3$ helices and allosteric site guarding loop5 (L5) (Figure 2A all panels; only **3k** has been shown for pictorial clarity).

Earlier research works suggest the ADP bound conformation of Eg5 Kinesin is structurally more dynamic compared to that of the ATP bound conformational state. In particular, the flexibility of the Switch-I (amino acids: 229−234) region is responsible for the release of ADP[27] (the end product of previous reaction cycle) and subsequent binding of incoming ATP. The structural stability of the Switch-I region in the ATP bound conformation of the Eg5 motor domain stems from the proper positioning of switch-I amino acid residues (Ser233, Arg234) to stabilize the scissile γ-phosphate group of incoming ATP as well as to activate the water nucleophile needed for ATP hydrolysis.[28] Other than the direct catalytic role of the switch-I region, it also plays crucial role in structuring the switch-II region (amino acids: 265−277), which in turn properly positions the microtubule binding $\alpha 4$ relay helix (amino acids: 278−302) of Eg5 kinesin to dock with α/β tubulin heterodimer. Therefore, the nucleotide-driven differential structural dispositions of the Switch-I and Switch-II regions of Eg5 kinesin play a pivotal role in its microtubule gliding activity. Importantly, just like the other monastrol binding site targeting allosteric inhibitors, the synthesized BIM derivatives **3k** and **3b** freeze the ADP bound conformation of the Eg5 motor domain by inhibiting the structural transition of the $\alpha 3$ helix needed to release ADP as well as to accept the γ-phosphate group of incoming ATP (Figure 2B all panels; only **3k** has been shown for pictorial clarity). In addition, MD simulation analysis divulges **3k** binding to Eg5 motor domain in the presence of bound ADP decreases flexibilities of Switch-I and Switch-II regions compared to only the ADP bound conformation (Figure S2). In the Eg5/ADP/**3k** complex, the reduced flexibilities of switch-I, switch-II and tubulin binding $\alpha 4$ relay helix mimics the ATP bound Eg5 conformation,[73,74] which would ultimately lock the Eg5 in ADP bound state. Altogether, on the basis of these observations, we propose that the synthesized BIM derivatives **3k** and **3b** would exert Eg5 inhibitory activity by uncoupling the nucleotide driven conformational changes needed for Eg5 microtubule gliding.

CONCLUSIONS

In summary, we have reported an unprecedented approach for the first time to access functionalized derivatives of BIMs in an excellent yield via taurine-catalyzed condensation of structurally diverse aldehydes with indole in water medium. This catalytic application has been proven active under milder reaction conditions, providing broad substrate scope toward accessing varied targeted BIMs for their biological evaluation. Furthermore, a detailed in silico based structure activity evaluation of the synthesized BIM derivatives demonstrates their potential to bind the allosteric inhibitory site of kinesin Eg5, a well-established anticancer drug target protein. The molecular mechanism of synthesized BIM derivative mediated allosteric inhibition of Eg5 kinesin clearly demonstrates their ability to lock Eg5 gliding on a microtubule track. The inhibition mechanism is similar to the previously reported Eg5 inhibitors under clinical trials. However, compared to the previously reported allosteric inhibitors, the superior Eg5 binding efficiency of synthesized BIM derivatives and their unique ability to cope with drug-resistant Eg5 mutations confer immense promise for their use as resistance-resistant antineoplastic therapeutic leads. Overall, the procedure's simplicity and straightforward operational methodology make it an outstanding strategy for these intriguing and appealing reaction products, which continue to be in high demand. Further, in the search for potent drug candidates, an effort toward the construction of bioactive BIMs and obtaining its advanced biological data is ongoing and will be disclosed in due course.

ASSOCIATED CONTENT

ⓈI Supporting Information

The Supporting Information is available free of charge at https://pubs.acs.org/doi/10.1021/acsomega.1c07258.

> Experimental procedures, full characterization for all new compounds, in silico evaluation of all compounds, and Table S1 (PDF)

AUTHOR INFORMATION

Corresponding Authors

Sudipta Bhattacharyya − Department of Bioscience and Bioengineering, Indian Institute of Technology Jodhpur, Jodhpur 342037, India; Email: rd.erande@iitj.ac

Rohan D. Erande − Department of Chemistry, Indian Institute of Technology Jodhpur, Jodhpur 342037, India; ⓞ orcid.org/0000-0002-8763-5353; Email: sudipta@iitj.ac.in

Authors

Kailas A. Chavan − Department of Chemistry, Indian Institute of Technology Jodhpur, Jodhpur 342037, India

Manjari Shukla − Department of Bioscience and Bioengineering, Indian Institute of Technology Jodhpur, Jodhpur 342037, India

Amar Nath Singh Chauhan − Department of Chemistry, Indian Institute of Technology Jodhpur, Jodhpur 342037, India

Sushobhan Maji − Department of Bioscience and Bioengineering, Indian Institute of Technology Jodhpur, Jodhpur 342037, India

Ghanshyam Mali − Department of Chemistry, Indian Institute of Technology Jodhpur, Jodhpur 342037, India

Complete contact information is available at:

■ REFERENCES

(1) Safe, S.; Papineni, S.; Chintharlapalli, S. Cancer Chemotherapy with Indole-3-Carbinol, Bis(3′-Indolyl)Methane and Synthetic Analogs. *Cancer Lett.* **2008**, *269* (2), 326−338.

(2) Imran, S.; Taha, M.; Ismail, N. A Review of Bisindolylmethane as an Important Scaffold for Drug Discovery. *Curr. Med. Chem.* **2015**, *22* (38), 4412−4433.

(3) Chao, W.-R.; Yean, D.; Amin, K.; Green, C.; Jong, L. Computer-Aided Rational Drug Design: A Novel Agent (SR13668) Designed to Mimic the Unique Anticancer Mechanisms of Dietary Indole-3-Carbinol to Block Akt Signaling. *J. Med. Chem.* **2007**, *50* (15), 3412−3415.

(4) Praveen, P.; Parameswaran, P.; Majik, M. Bis(Indolyl)Methane Alkaloids: Isolation, Bioactivity, and Syntheses. *Synthesis* **2015**, *47* (13), 1827−1837.

(5) Mhaldar, S. N.; Mandrekar, K. S.; Gawde, M. K.; Shet, R. V.; Tilve, S. G. Solventless Mechanosynthesis Of *Bis* (Indolyl)Methanes. *Synth. Commun.* **2019**, *49* (1), 94−101.

(6) Jella, R. R.; Nagarajan, R. Synthesis of Indole Alkaloids Arsindoline A, Arsindoline B and Their Analogues in Low Melting Mixture. *Tetrahedron* **2013**, *69* (48), 10249−10253.

(7) Wati, F. A.; Santoso, M.; Moussa, Z.; Fatmawati, S.; Fadlan, A.; Judeh, Z. M. A. Chemistry of Trisindolines: Natural Occurrence, Synthesis and Bioactivity. *RSC Adv.* **2021**, *11* (41), 25381−25421.

(8) Devi, T. J.; Singh, T. P.; Singh, R. R.; Sharma, K. G.; Singh, O. M. Synthesis of Tri-Indolylmethane Derivatives Using a Deep Eutectic Solvent. *Russ J. Org. Chem.* **2021**, *57* (2), 255−264.

(9) Fang, S.-Y.; Chen, S.-Y.; Chen, Y.-Y.; Kuo, T.-J.; Wen, Z.-H.; Chen, Y.-H.; Hwang, T.-L.; Sung, P.-J. Natural Indoles From the Bacterium *Pseudovibrio Denitrificans* P81 Isolated From a Marine Sponge, *Aaptos* Species. *Nat. Prod. Commun.* **2021**, *16* (9), 1934578X2110337.

(10) Kobayashi, M.; Aoki, S.; Gato, K.; Matsunami, K.; Kurosu, M.; Kitagawa, I. Marine Natural Products. XXXIV. Trisindoline, a New Antibiotic Indole Trimer, Produced by a Bacterium of Vibrio Sp. Separated from the Marine Sponge Hyrtios Altum. *Chem. Pharm. Bull.* **1994**, *42* (12), 2449−2451.

(11) Shiri, M.; Zolfigol, M. A.; Kruger, H. G.; Tanbakouchian, Z. Bis- and Trisindolylmethanes (BIMs and TIMs). *Chem. Rev.* **2010**, *110* (4), 2250−2293.

(12) Nagre, D. T.; Mali, S. N.; Thorat, B. R.; Thorat, S. A.; Chopade, A. R.; Farooqui, M.; Agrawal, B. Synthesis, In-Silico Potential Enzymatic Target Predictions, Pharmacokinetics, Toxicity, Anti-Microbial and Anti-Inflammatory Studies of Bis-(2-Methylindolyl) Methane Derivatives. *Curr. Enzyme Inhib.* **2021**, *17* (2), 127−143.

(13) Zhang, M.-Z.; Chen, Q.; Yang, G.-F. A Review on Recent Developments of Indole-Containing Antiviral Agents. *Eur. J. Med. Chem.* **2015**, *89*, 421−441.

(14) Bharate, S. B.; Bharate, J. B.; Khan, S. I.; Tekwani, B. L.; Jacob, M. R.; Mudududdla, R.; Yadav, R. R.; Singh, B.; Sharma, P. R.; Maity, S.; Singh, B.; Khan, I. A.; Vishwakarma, R. A. Discovery of 3,3′-Diindolylmethanes as Potent Antileishmanial Agents. *Eur. J. Med. Chem.* **2013**, *63*, 435−443.

(15) Li, Y.; Kong, D.; Ahmad, A.; Bao, B.; Sarkar, F. H. Antioxidant Function of Isoflavone and 3,3′-Diindolylmethane: Are They Important for Cancer Prevention and Therapy? *Antioxid. Redox Signaling* **2013**, *19* (2), 139−150.

(16) Lu, L.; Jiang, M.; Zhu, C.; He, J.; Fan, S. Amelioration of Whole Abdominal Irradiation-Induced Intestinal Injury in Mice with 3,3′-Diindolylmethane (DIM). *Free Radical Biol. Med.* **2019**, *130*, 244−255.

(17) Rzemieniec, J.; Wnuk, A.; Lasoń, W.; Bilecki, W.; Kajta, M. The Neuroprotective Action of 3,3′-Diindolylmethane against Ischemia Involves an Inhibition of Apoptosis and Autophagy That Depends on HDAC and AhR/CYP1A1 but Not ERα/CYP19A1 Signaling. *Apoptosis* **2019**, *24* (5−6), 435−452.

(18) Mari, M.; Tassoni, A.; Lucarini, S.; Fanelli, M.; Piersanti, G.; Spadoni, G. Brønsted Acid Catalyzed Bisindolization of α-Amido Acetals: Synthesis and Anticancer Activity of Bis(Indolyl)Ethanamino Derivatives: Brønsted Acid Catalyzed Bisindolization of α-Amido Acetals. *Eur. J. Org. Chem.* **2014**, *2014* (18), 3822−3830.

(19) Deb, B.; Debnath, S.; Chakraborty, A.; Majumdar, S. Bis-Indolylation of Aldehydes and Ketones Using Silica-Supported FeCl₃ : Molecular Docking Studies of Bisindoles by Targeting SARS-CoV-2 Main Protease Binding Sites. *RSC Adv.* **2021**, *11* (49), 30827−30839.

(20) Andreani, A.; Burnelli, S.; Granaiola, M.; Leoni, A.; Locatelli, A.; Morigi, R.; Rambaldi, M.; Varoli, L.; Landi, L.; Prata, C. Antitumor Activity of Bis-Indole Derivatives. *J. Med. Chem.* **2008**, *51* (15), 4563−4570.

(21) Panov, A. A.; Lavrenov, S. N.; Mirchink, E. P.; Isakova, E. B.; Korolev, A. M.; Trenin, A. S. Synthesis and Antibacterial Activity of Novel Arylbis(Indol-3-Yl)Methane Derivatives. *J. Antibiot.* **2021**, *74* (3), 219−224.

(22) Tian, X.; Liu, K.; Zu, X.; Ma, F.; Li, Z.; Lee, M.; Chen, H.; Li, Y.; Zhao, Y.; Liu, F.; Oi, N.; Bode, A. M.; Dong, Z.; Kim, D. J. 3,3′-Diindolylmethane Inhibits Patient-Derived Xenograft Colon Tumor Growth by Targeting COX1/2 and ERK1/2. *Cancer Lett.* **2019**, *448*, 20−30.

(23) Lee, J. 3,3′-Diindolylmethane Inhibits TNF-α- and TGF-β-Induced Epithelial−Mesenchymal Transition in Breast Cancer Cells. *Nutr. Cancer* **2019**, *71* (6), 992−1006.

(24) Kim, S. Cellular and Molecular Mechanisms of 3,3′-Diindolylmethane in Gastrointestinal Cancer. *Int. J. Mol. Sci.* **2016**, *17* (7), 1155.

(25) Kim, J. Y.; Le, T. A. N.; Lee, S. Y.; Song, D.-G.; Hong, S.-C.; Cha, K. H.; Lee, J. W.; Pan, C.-H.; Kang, K. 3,3′-Diindolylmethane Improves Intestinal Permeability Dysfunction in Cultured Human Intestinal Cells and the Model Animal *Caenorhabditis Elegans*. *J. Agric. Food Chem.* **2019**, *67* (33), 9277−9285.

(26) Kong, D.; Li, Y.; Wang, Z.; Banerjee, S.; Sarkar, F. H. Inhibition of Angiogenesis and Invasion by 3,3′-Diindolylmethane Is Mediated by the Nuclear Factor−KB Downstream Target Genes *MMP-9* and *UPA* That Regulated Bioavailability of Vascular Endothelial Growth Factor in Prostate Cancer. *Cancer Res.* **2007**, *67* (7), 3310−3319.

(27) Chang, X. 3,3′-Diindolylmethane Inhibits Angiogenesis and the Growth of Transplantable Human Breast Carcinoma in Athymic Mice. *Carcinogenesis* **2005**, *26* (4), 771−778.

(28) Abid, O.; Imran, S.; Taha, M.; Ismail, N. H.; Jamil, W.; Kashif, S. M.; Khan, K. M.; Yusoff, J. Synthesis, β-Glucuronidase Inhibition and Molecular Docking Studies of Cyano-Substituted Bisindole Hydrazone Hybrids. *Mol. Diversity* **2021**, *25* (2), 995−1009.

(29) Bal, T. R.; Anand, B.; Yogeeswari, P.; Sriram, D. Synthesis and Evaluation of Anti-HIV Activity of Isatin β-Thiosemicarbazone Derivatives. *Bioorg. Med. Chem. Lett.* **2005**, *15* (20), 4451−4455.

(30) Jiang, Y.; Fang, Y.; Ye, Y.; Xu, X.; Wang, B.; Gu, J.; Aschner, M.; Chen, J.; Lu, R. Anti-Cancer Effects of 3, 3′-Diindolylmethane on Human Hepatocellular Carcinoma Cells Is Enhanced by Calcium Ionophore: The Role of Cytosolic Ca2+ and P38 MAPK. *Front. Pharmacol.* **2019**, *10*, 1167.

(31) Marrelli, M.; Cachet, X.; Conforti, F.; Sirianni, R.; Chimento, A.; Pezzi, V.; Michel, S.; Statti, G. A.; Menichini, F. Synthesis of a New Bis(Indolyl)Methane That Inhibits Growth and Induces Apoptosis in Human Prostate Cancer Cells. *Nat. Prod. Res.* **2013**, 27 (21), 2039−2045.

(32) Nachshon-Kedmi, M.; Yannai, S.; Fares, F. A. Induction of Apoptosis in Human Prostate Cancer Cell Line, PC3, by 3,3′-Diindolylmethane through the Mitochondrial Pathway. *Br. J. Cancer* **2004**, 91 (7), 1358−1363.

(33) Pandey, K. P.; Rahman, M. T.; Cook, J. M. Bisindole Alkaloids from the Alstonia Species: Recent Isolation, Bioactivity, Biosynthesis, and Synthesis. *Molecules* **2021**, 26 (11), 3459.

(34) Khanna, L.; Mansi; Yadav, S.; Misra, N.; Khanna, P. In Water" Synthesis of Bis(Indolyl)Methanes: A Review. *Synth. Commun.* **2021**, 51 (19), 2892−2923.

(35) Paira, P.; Hazra, A.; Kumar, S.; Paira, R.; Sahu, K. B.; Naskar, S.; Mondal, S.; Maity, A.; Banerjee, S.; Mondal, N. B. Efficient Synthesis of 3, 3-Diheteroaromatic Oxindole Analogues and Their in Vitro Evaluation for Spermicidal Potential. *Bioorg. Med. Chem. Lett.* **2009**, 19 (16), 4786−4789.

(36) Hassani Bagheri, F.; Khabazzadeh, H.; Fayazi, M. Copper-Catalyzed N-Arylation of Bis(Indolyl)Methanes: The First Approach for the Synthesis of Unsymmetrical N-Aryl Bis(Indolyl)Methanes by C−N Cross-Coupling Reaction. *C. R. Chim.* **2021**, 24 (2), 305−317.

(37) Talukdar, D.; Thakur, A. J. A Green Synthesis of Symmetrical Bis(Indol-3-Yl)Methanes Using Phosphate-Impregnated Titania Catalyst under Solvent Free Grinding Conditions. *Green Chem. Lett. Rev.* **2013**, 6 (1), 55−61.

(38) Yuan, Z.; Chen, S.; Weng, Z. Copper-Catalyzed Synthesis of Trifluoromethylated Bis(Indolyl)Arylmethanes from 2-Arylindoles and 2,2,2-Trifluoroacetohydrazide. *Org. Chem. Front.* **2020**, 7 (3), 482−486.

(39) Ling, Y.; An, D.; Zhou, Y.; Rao, W. Ga(OTf)₃-Catalyzed Temperature-Controlled Regioselective Friedel−Crafts Alkylation of Trifluoromethylated 3-Indolylmethanols with 2-Substituted Indoles: Divergent Synthesis of Trifluoromethylated Unsymmetrical 3,3′-and 3,6′-Bis(Indolyl)Methanes. *Org. Lett.* **2019**, 21 (9), 3396−3401.

(40) Du, K.-S.; Huang, J.-M. Electrochemical Synthesis of Bisindolylmethanes from Indoles and Ethers. *Org. Lett.* **2018**, 20 (10), 2911−2915.

(41) Radfar, I.; Miraki, M. K.; Ghandi, L.; Esfandiary, N.; Abbasi, S.; Karimi, M.; Heydari, A. BF₃-Grafted Fe₃O₄@Sucrose Nanoparticles as a Highly-Efficient Acid Catalyst for Syntheses of Dihydroquinazolinones (DHQZs) and Bis 3-Indolyl Methanes (BIMs): BF3-Grafted Fe3O4@Sucrose Nanoparticles. *Appl. Organomet. Chem.* **2018**, 32 (8), e4431.

(42) Shirini, F.; Langroodi, M. S.; Abedini, M. Efficient Synthesis of Bis (Indolyl) Methanes Catalyzed by (PhCH2PPh3)+Br3− under Solvent-Free Conditions. *Chin. Chem. Lett.* **2010**, 21 (11), 1342−1345.

(43) Nadkarni, S. V.; Gawande, M. B.; Jayaram, R. V.; Nagarkar, J. M. Synthesis of Bis(Indolyl)Methanes Catalyzed by Surface Modified Zirconia. *Catal. Commun.* **2008**, 9 (8), 1728−1733.

(44) Sarrafi, Y.; Alimohammadi, K.; Sadatshahabi, M.; Norozipoor, N. An Improved Catalytic Method for the Synthesis of 3, 3-Di (Indolyl) Oxindoles Using Amberlyst 15 as a Heterogeneous and Reusable Catalyst in Water. *Monatsh. Chem.* **2012**, 143 (11), 1519−1522.

(45) Chakrabarty, M.; Sarkar, S.; Harigaya, Y. A Facile Clay-Mediated Synthesis of 3, 3-Diindolyl-2-Indolinones from Isatins. *J. Chem. Res.* **2005**, 2005 (8), 540−542.

(46) Sharma, R.; Sharma, C. A Highly Efficient Synthesis of Oxindoles Using a Functionalized Silica Gel as Support for Indium (III) Acetylacetonate Catalyst in an Aqueous-Acetonitrile Medium. *J. Mol. Catal. A: Chem.* **2010**, 332 (1−2), 53−58.

(47) Matzkeit, Y. H.; Tornquist, B. L.; Manarin, F.; Botteselle, G. V.; Rafique, J.; Saba, S.; Braga, A. L.; Felix, J. F.; Schneider, R. Borophosphate Glasses: Synthesis, Characterization and Application as Catalyst for Bis(Indolyl)Methanes Synthesis under Greener Conditions. *J. Non-Cryst. Solids* **2018**, 498, 153−159.

(48) Heravi, M. M.; Zakeri, M.; Karimi, N.; Saeedi, M.; Oskooie, H. A.; Tavakoli-Hosieni, N. Acidic Ionic Liquid [(CH2) 4SO3HMIM]-[HSO4]: A Green Media for the Simple and Straightforward Synthesis of 2, 4, 5-Trisubstituted Imidazoles. *Synth. Commun.* **2010**, 40 (13), 1998−2006.

(49) Rad-Moghadam, K.; Sharifi-Kiasaraie, M.; Taheri-Amlashi, H. Synthesis of Symmetrical and Unsymmetrical 3, 3-Di (Indolyl) Indolin-2-Ones under Controlled Catalysis of Ionic Liquids. *Tetrahedron* **2010**, 66 (13), 2316−2321.

(50) Inamdar, S. M.; Gonnade, R. G.; Patil, N. T. Synthesis of Annulated Bis-Indoles through Au(i)/Brønsted Acid-Catalyzed Reactions of (1H-Indol-3-Yl)(Aryl)Methanols with 2-(Arylethynyl)-1H-Indoles. *Org. Biomol. Chem.* **2017**, 15 (4), 863−869.

(51) Xie, X.; Du, X.; Chen, Y.; Liu, Y. One-Pot Synthesis of Indole-Fused Scaffolds via Gold-Catalyzed Tandem Annulation Reactions of 1,2-Bis(Alkynyl)-2-En-1-Ones with Indoles. *J. Org. Chem.* **2011**, 76 (21), 9175−9181.

(52) Dethe, D. H.; Erande, R. D.; Dherange, B. D. Remarkable Switch of Regioselectivity in Diels−Alder Reaction: Divergent Total Synthesis of Borreverine, Caulindoles, and Flinderoles. *Org. Lett.* **2014**, 16 (10), 2764−2767.

(53) Dethe, D. H.; Erande, R. D.; Ranjan, A. Biomimetic Total Syntheses of Borreverine and Flinderole Alkaloids. *J. Org. Chem.* **2013**, 78 (20), 10106−10120.

(54) Dethe, D. H.; Erande, R. D.; Ranjan, A. Biomimetic Total Syntheses of Flinderoles B and C. *J. Am. Chem. Soc.* **2011**, 133 (9), 2864−2867.

(55) Abd El Aleem Ali Ali El-Remaily, M.; Elhady, O. M. Green Bio-organic and Recoverable Catalyst Taurine (2-aminoethanesulfonic Acid) for Synthesis of Bio-active Compounds 3,4-Dihydropyrimidin Derivatives in Aqueous Medium. *ChemistrySelect* **2020**, 5 (39), 12098−12102.

(56) Heck, M. M.; Pereira, A.; Pesavento, P.; Yannoni, Y.; Spradling, A. C.; Goldstein, L. S. The Kinesin-like Protein KLP61F Is Essential for Mitosis in Drosophila. *J. Cell Biol.* **1993**, 123 (3), 665−679.

(57) Sawin, K. E.; LeGuellec, K.; Philippe, M.; Mitchison, T. J. Mitotic Spindle Organization by a Plus-End-Directed Microtubule Motor. *Nature* **1992**, 359 (6395), 540−543.

(58) Waitzman, J. S.; Rice, S. E. Mechanism and Regulation of Kinesin-5, an Essential Motor for the Mitotic Spindle: Kinesin-5 Mechanism and Regulation. *Biol. Cell* **2014**, 106 (1), 1−12.

(59) Kashina, A.; Rogers, G. C.; Scholey, J. The BimC Family of Kinesins: Essential Bipolar Mitotic Motors Driving Centrosome Separation. *Biochim. Biophys. Acta, Mol. Cell Res.* **1997**, 1357 (3), 257−271.

(60) Rice, S.; Lin, A. W.; Safer, D.; Hart, C. L.; Naber, N.; Carragher, B. O.; Cain, S. M.; Pechatnikova, E.; Wilson-Kubalek, E. M.; Whittaker, M. A Structural Change in the Kinesin Motor Protein That Drives Motility. *Nature* **1999**, 402 (6763), 778−784.

(61) Goulet, A.; Behnke-Parks, W. M.; Sindelar, C. V.; Major, J.; Rosenfeld, S. S.; Moores, C. A. The Structural Basis of Force Generation by the Mitotic Motor Kinesin-5. *J. Biol. Chem.* **2012**, 287 (53), 44654−44666.

(62) Yan, Y.; Sardana, V.; Xu, B.; Homnick, C.; Halczenko, W.; Buser, C. A.; Schaber, M.; Hartman, G. D.; Huber, H. E.; Kuo, L. C. Inhibition of a Mitotic Motor Protein: Where, How, and Conformational Consequences. *J. Mol. Biol.* **2004**, 335 (2), 547−554.

(63) Ulaganathan, V.; Talapatra, S. K.; Rath, O.; Pannifer, A.; Hackney, D. D.; Kozielski, F. Structural Insights into a Unique Inhibitor Binding Pocket in Kinesin Spindle Protein. *J. Am. Chem. Soc.* **2013**, 135 (6), 2263−2272.

(64) Zhang, W.; Zhai, L.; Lu, W.; Boohaker, R. J.; Padmalayam, I.; Li, Y. Discovery of Novel Allosteric Eg5 Inhibitors Through Structure-Based Virtual Screening. *Chem. Biol. Drug Des.* **2016**, 88 (2), 178−187.

(65) Indorato, R.-L.; Talapatra, S. K.; Lin, F.; Haider, S.; Mackay, S. P.; Kozielski, F.; Skoufias, D. A. Is the Fate of Clinical Candidate

Arry-520 Already Sealed? Predicting Resistance in Eg5−Inhibitor Complexes. *Mol. Cancer Ther.* **2019**, *18* (12), 2394−2406.

(66) Mali, G.; Shaikh, B. A.; Garg, S.; Kumar, A.; Bhattacharyya, S.; Erande, R. D.; Chate, A. V. Design, Synthesis, and Biological Evaluation of Densely Substituted Dihydropyrano[2,3-*c*]Pyrazoles *via* a Taurine-Catalyzed Green Multicomponent Approach. *ACS Omega* **2021**, *6* (45), 30734−30742.

(67) Subba Reddy, B.V.; Rajeswari, N.; Sarangapani, M.; Prashanthi, Y.; Ganji, R. J.; Addlagatta, A. Iodine-Catalyzed Condensation of Isatin with Indoles: A Facile Synthesis of Di (Indolyl) Indolin-2-Ones and Evaluation of Their Cytotoxicity. *Bioorg. Med. Chem. Lett.* **2012**, *22* (7), 2460−2463.

(68) Kamal, A.; Srikanth, Y. V. V.; Khan, M. N. A.; Shaik, T. B.; Ashraf, Md. Synthesis of 3,3-Diindolyl Oxyindoles Efficiently Catalysed by FeCl3 and Their in Vitro Evaluation for Anticancer Activity. *Bioorg. Med. Chem. Lett.* **2010**, *20* (17), 5229−5231.

(69) Vine, K.; Matesic, L.; Locke, J.; Ranson, M.; Skropeta, D. Cytotoxic and Anticancer Activities of Isatin and Its Derivatives: A Comprehensive Review from 2000−2008. *Anti-Cancer Agents Med. Chem.* **2009**, *9* (4), 397−414.

(70) Daneshvar, N.; Shirini, F.; Langarudi, M. S. N.; Karimi-Chayjani, R. Taurine as a Green Bio-Organic Catalyst for the Preparation of Bio-Active Barbituric and Thiobarbituric Acid Derivatives in Water Media. *Bioorg. Chem.* **2018**, *77*, 68−73.

(71) Shirini, F.; Daneshvar, N. Introduction of Taurine (2-Aminoethanesulfonic Acid) as a Green Bio-Organic Catalyst for the Promotion of Organic Reactions under Green Conditions. *RSC Adv.* **2016**, *6* (111), 110190−110205.

(72) Algarín, E. M.; Hernández-García, S.; Garayoa, M.; Ocio, E. M. Filanesib for the Treatment of Multiple Myeloma. *Expert Opin. Invest. Drugs* **2020**, *29* (1), 5−14.

(73) Parke, C. L.; Wojcik, E. J.; Kim, S.; Worthylake, D. K. ATP Hydrolysis in Eg5 Kinesin Involves a Catalytic Two-Water Mechanism. *J. Biol. Chem.,* **2010** *285* (8), 5859−5867.

(74) Ogunwa, T. H.; Laudadio, E.; Galeazzi, R.; Miyanishi, T. Insights into the Molecular Mechanisms of Eg5 Inhibition by (+)-Morelloflavone. *Pharmaceuticals* **2019**, *12* (2), 58.